In: 30th AIAA/CEAS Aeroacoustics Conference (2024), 04-07 June 2024, Rome, Italy, Article number 2024-3310
DOI: 10.2514/6.2024-3310

Prediction of far-field noise from installed corrugated nozzles

Francisco J. de Souza*† and Jack L. T. Lawrence‡
Institute of Sound and Vibration Research, University of Southampton, Southampton, SO17 1BJ, UK

Ricardo H. Cruz§ and Anderson R. Proença¶‖
School of Aerospace, Transport and Manufacturing, Cranfield University, Cranfield, MK43 0AL, UK

In this study, a reduced order model, devised by Lyu and Dowling, is used to predict the far-field installation noise of corrugated nozzles installed beneath a NACA aerofoil. A complementary investigation, detailed in another paper, reveals that employing square corrugations near the nozzle lip diminishes jet-surface interaction (JSI) noise compared to a round 40-mm diameter nozzle. This reduction is particularly notable for Strouhal numbers ranging from 0.3 to 0.9 and at high polar angles. The near-field pressure data, required for Lyu and Dowling's model, is gathered using a circular array consisting of eight 1/8-inch microphones in the Doak Laboratory, at the University of Southampton, UK. Generally, the predictions align well with the experimental trends for Mach numbers ranging from 0.4 to 1 under static ambient flow conditions. Furthermore, it is observed that a minimum of four azimuthal modes must be available to accurately predict the noise generated by the corrugated nozzles. The effects of free-stream Mach number, particularly focusing on the predictive capacity of Lyu and Dowling's model, are also investigated. Quantitative agreement at Strouhal numbers between 0.1 and 0.5 in evidenced.

I. Introduction

Jet engine noise reduction remains a significant concern in the aviation industry. As the bypass ratio of modern turbofan engines continues to increase, the proximity between the wing and the engine in underwing installations tends to aggravate the noise generation due to jet-surface interaction (JSI). Essentially, there is a noise scattering effect caused by the interaction between the jet hydrodynamic near-field with the nearby surface.

Among various strategies, passive exhaust lip treatments have gained considerable attention for their potential to reduce mixing noise, and possibly JSI noise. Serrations on exhaust nozzles, commonly referred to as chevrons, have proven to be an effective strategy for reducing jet mixing noise among various noise reduction techniques. Essentially, chevrons introduce streamwise vorticity, which in turn increases flow mixing near the nozzle and shifts acoustic energy from low to high frequencies. Chevrons exhibit the capability to specifically diminish low-frequency noise, particularly in downstream polar angles.[1],[2],[3]. Despite their effectiveness, chevrons are known to reduce the engine thrust because of the additional mixing. Therefore, there is a keen interest in developing treatments to reduce both mixing and JSI noise while minimizing their negative impact on engine performance.

In this sense, other geometric modifications to exhaust nozzle lips have been explored as a means to mitigate both jet mixing and JSI noise [2, 4–7]. Another example of such lip treatment is the use of square corrugations [7], whose noise features are investigated experimentally in a companion paper. Such techniques aim to mitigate both mixing and JSI noise without significantly compromising engine performance, i.e., causing loss of thrust.

To ensure that increasingly strict legislation requirements will be met with minimal aircraft performance penalty, the capacity to predict the JSI noise is crucial. Although advanced techniques such as LES can effectively tackle this problem, they are still computationally expensive for optimization or design. This is especially true at preliminary design stages, as the timescales are in the order of hours. Another restriction is their use in Multidisciplinary Optimization (MDO), which is commonplace in aircraft design, and also demands quick turnaround times.

*Visiting Fellow, ISVR, University of Southampton
†Lecturer, School of Mechanical Engineering, Federal University of Uberlandia, Brazil.
‡Senior Research Fellow in Experimental Aeroacoustics, ISVR, University of Southampton, AIAA Member.
§MSc candidate in Aerospace Dynamics, Centre for Aeronautics, Cranfield University
¶Lecturer in Aerodynamics, Applied Aerodynamics Group, Cranfield University, AIAA Member.
‖Visiting Fellow, Acoustics Group, University of Southampton

In response to the demand for faster predictive methods, numerous previous contributions have subsidized the development of so-called reduced order methods for predicting jet-surface interaction (JSI) noise. Of particular interest in this paper is the model proposed by Lyu and Dowling [8], which has been shown to be accurate and robust. Nonetheless, it requires the jet hydrodynamic pressure field as input. In this paper, the latter, as measured in the Doak Laboratory using a circular array of eight microphones strategically positioned downstream of the nozzle, is used as input.

The primary aim of this study is to evaluate the reliability and robustness of Lyu and Dowling's model when dealing with subtle geometric alterations at the nozzle exit, under both static and in-flight conditions. Despite the uncertainties and approximations inherent in our approach, we find the results to be satisfactory for providing initial estimates and for comparing various geometric configurations in terms of installation noise.

II. Methods

Experiments were carried out in the Doak Laboratory using the Flight Jet Rig (FJR).A NACA4415-profiled wing model and two types of nozzle - a baseline round nozzle and four square corrugated lip-modified nozzles with varying degrees of flow penetration - were investigated. Details concerning the hardware and instrumentation used in the experiments are described below.

A. Experiments

The Doak Laboratory comprises a chamber, fully anechoic above 400 Hz, with dimensions approximately equal to 15 m-long, 7 m-wide and 5 m-high. Two separate air supply systems allow in-flight simulations of single stream jet flows using the FJR. The primary 'core' jet flow is supplied by a high-pressure compressor-reservoir system, capable of producing a maximum inlet pressure of 20 Bar. The secondary 'flight' flow is supplied by a 1.1 pressure ratio fan. The 300 mm-diameter flight nozzle can produce flow velocities up to 100 m/s. The present paper deals with both static and in-flight cases.

Total temperature and both total and static pressure sensors are mounted both in the plenum (located far upstream of the nozzle exit) and along the pipework of the core and flight jet ducts. Ambient chamber properties, such as pressure, temperature and relative humidity, are also recorded. These readings are required to set the nominal nozzle exit acoustic Mach number operating conditions and to apply corrections to the data (e.g. atmospheric attenuation and NPR variation during long hot-wire traverse measurements). Far-field data were obtained using a linear "flyover" array. Ten microphones were used to cover polar observer angles ranging from 40° to 130°, at 10° intervals. The closest microphone, $\theta = 90°$, was located at approximately 55 jet nozzle diameters from the nozzle centreline. An image of the anechoic chamber depicting the FJR and the far-field microphone array, from which the data presented in this report was recorded, is shown in Fig. 1(a). Near-field measurements were also recorded using an eight-microphone azimuthal array, illustrated in Fig. 1(b).

For the installed tests, a 2-D aerofoil (uniform chord in the spanwise direction) was mounted next to each nozzle. This aerofoil was designed using a NACA4415 profile and has a chord length of $c = 150$ mm and span $b = 600$ mm. The aerofoil was 3-D printed in three sections and later assembled using two internal threaded studs to ensure rigidity. The aerofoil trailing edge (TE) was located at $L/D = 3$ and $H/D = 0.6$, where L was the axial distance between the nozzle exit plane and the aerofoil TE and H was the vertical distance between the jet centreline and the aerofoil TE. The wing angle of attack for the present experiments was set at $\alpha = 4°$. The baseline round nozzle used in this work was a 40mm-diameter round, convergent nozzle [7, 9] with a convergence half-angle of 2.4°. The geometry close to the nozzle lip was modified using square corrugations varying along the nozzle lip circumference. The penetration angle was varied between 3, 6, 9 and 12 degrees and was kept constant for both 'internal' and 'external' surfaces. Thus, the effective area at the nozzle exit was exactly the same as the baseline (i.e., $A = 1257$ mm^2), neglecting viscous effects. The number of complete corrugations in this study was set at 16.

Three test campaigns were conducted in total: (1) far-field acoustic, (2) azimuthal hydrodynamic near-field, and (3) two-component unsteady velocity field. The far-field acoustic test was performed for both isolated and installed jet configurations. Data from three nominal jet exit acoustic Mach numbers were recorded ($M = 0.4$, $M = 0.6$ and $M = 0.8$) for the isolated nozzles, while experiments at $M = 0.6$ were carried out for the installed jets.

All data were acquired using a 24-bit National Instruments dynamic signal acquisition system. Each test point was recorded for ten seconds at a sampling rate of 200k samples per second. The microphones were calibrated before and after the test campaign. The voltage data acquired by each microphone were converted to a free-field pressure using a frequency-dependent sensitivity transfer function obtained during the calibration procedure. Each signal was also corrected for amplifier gain, atmospheric attenuation and then normalised to a distance of 1m (assuming linear spherical

propagation physics).

Power spectral density information was obtained using Welch's method and the final sound pressure levels were computed using a reference pressure of 20 μPa. Overall sound pressure levels were obtained by integrating the sound pressure levels (SPL) values between $0.1 \leq St \leq 10$, rather than using the root-mean-square of the entire time signal in order to avoid the contaminated energy beyond the low and high frequency data limits.

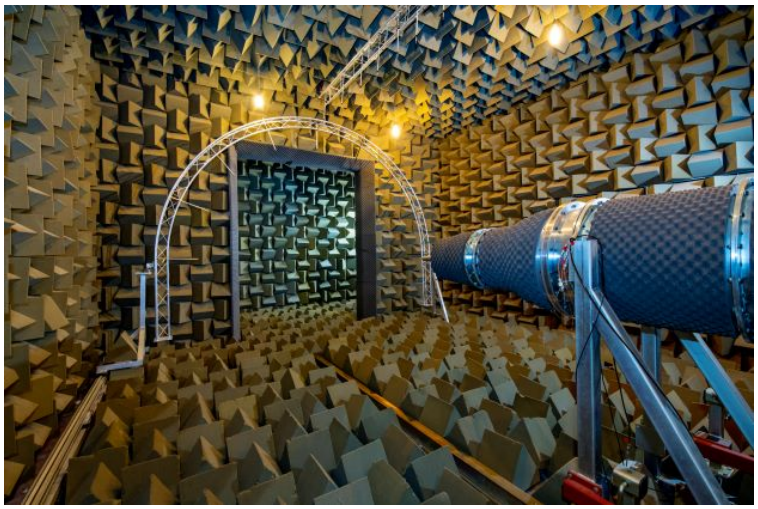

(a) Far-field measurements

(b) Near-field measurements

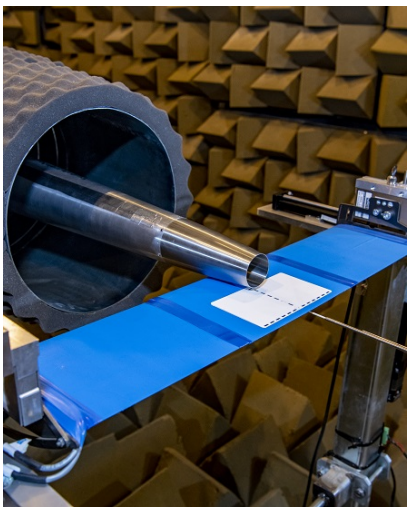

(c) Flowfield measurements

Fig. 1 ISVR Doak Laboratory, located at the University of Southampton, UK

B. Numerical model

Lyu and Dowling's model, as delineated in [8], was incorporated into an in-house code, referred to as DQ, in conjunction with empirical adjustments for free-stream velocity corrections, as described in [[10]. Initially, experimental near-field pressure data must undergo azimuthal mode decomposition to serve as input for the DQ code. Subsequently, the resulting modal sound pressure levels, together with operational parameters and geometric information, are utilized to predict the installed far-field noise. Further details on this process can be found in [8] and [10].

Ideally, the near-field Sound Pressure Level (SPL) should be available at the aerofoil trailing edge position, $L/D = 3$ and $H = /D = 0.6$.

However, due to limitations in the experimental setup, near-field measurements could be taken only at $r/D = 1.1$ for

$x/D = -0.5, 0, 0.5, 1, 1.5, 2$ and 3, and at $r/D = 0.8$ for $x/D = -0.5, 0, 0.5, 1, 1.5$ and 2. Therefore, it was not possible to estimate the axial wave-numbers at $x/D = 3$ following the procedure described by [8], who assume that the near-field decays exponentially in the radial direction at a given axial position. This assumption is derived from wave-packet models. Instead, the axial wave-number (K_x) as a function of the Strouhal number (St) was estimated based on an empirical correlation established by [10]:

$$K_x = (2\pi/D)(0.1 + 1.4St) \tag{1}$$

These estimates were employed to extrapolate the near-field SPL, initially recorded at $r/D = 1.1$, to the aerofoil TE position $r/D = 0.6$ by modeling the hydrodynamic spectra radial decay as a Bessel function of the second kind ([8]).

For the in-flight predictions, we utilize another empirical correlation developed by [10] is employed. This correlation accounts for the effect of in-flight velocity on the near-field SPL measured under static conditions, and is incorporated via Eq. 2:

$$SPL_{inflight} = SPL_{static}((U_j - U_f)/U_j)^3 \tag{2}$$

III. Results and discussion

A. Predictions versus experiments for static cases

Since experimental data for the installed nozzle is only available at jet Mach number $M_j = 0.6$, all results presented in the current work refer to that specific condition.

To initially evaluate the accuracy of Lyu and Dowling's model, we examine the impact of the number of modes on the predictions of installed noise for nozzle SC12 (12 degrees penetration). As illustrated in Figure 2, it is evident that the predicted Sound Pressure Level (SPL) increases with the number of modes and generally aligns better with experimental data. Consequently, for all subsequent simulations, we opted for 5 modes. While typically 2 modes are adequate for predicting installation noise in round jets, the presence of non-axisymmetric jets like corrugations often redistributes energy among higher modes, necessitating this adjustment. Corrugations, akin to chevrons, induce the generation of streamwise vorticity.

Figure 3 displays both the measured and predicted spectra for corrugated nozzle SC03, showcasing data for polar angles of 90 and 130 degrees. Additionally, the experimental spectrum for the isolated jet is included for comparative analysis. It is observed that, predominantly, the sound pressure levels are under-predicted in comparison to the experimental results.

Figures 4, 5, and 6 depict the comparison for nozzles SC06, SC09, and SC12, respectively. Similar trends are observed across all cases. While there appears to be a horizontal shift in the predictions compared to the experimental data, the overall agreement above a Strouhal number of 0.2 is deemed satisfactory, considering the inherent limitations and uncertainties associated with the near-field measurements. It is worth noting that since the near-field pressure varies exponentially in the radial direction, even slight inaccuracies in the positioning of radial microphones can lead to greater inaccuracies in hydrodynamic pressure measurements.

Arguably, the implicit assumption that the axial wave-numbers remain constant, akin to those for a round nozzle, could influence the accuracy of such predictions. This is particularly crucial because the extrapolation of the near-field SPL from $r/D = 1.1$ to $r/D = 0.6$ elies heavily on precise estimates of the axial wave-numbers. These axial wave-numbers serve as arguments in exponential functions governing the decay of the hydrodynamic field [8]. However, predictions for the equivalent round nozzle, i.e., of the same diameter as the corrugated ones (as depicted in Fig. 7), reveal persistent under-predictions. Consequently, the utilization of an empirical correlation for the axial wave-numbers based on experiments with a round nozzle, for predicting installation noise of corrugated nozzles, appears to hold secondary significance.

An important finding is the model's capability to predict the relative difference in Sound Pressure Level (SPL) between various nozzles. Figure 8 corroborates this assertion. This observation holds significant implications, suggesting that Lyu and Dowling's model exhibits sensitivity to subtle geometric variations among nozzles. Consequently, it can serve as a dependable tool for swift predictions, provided that the near-field is available.

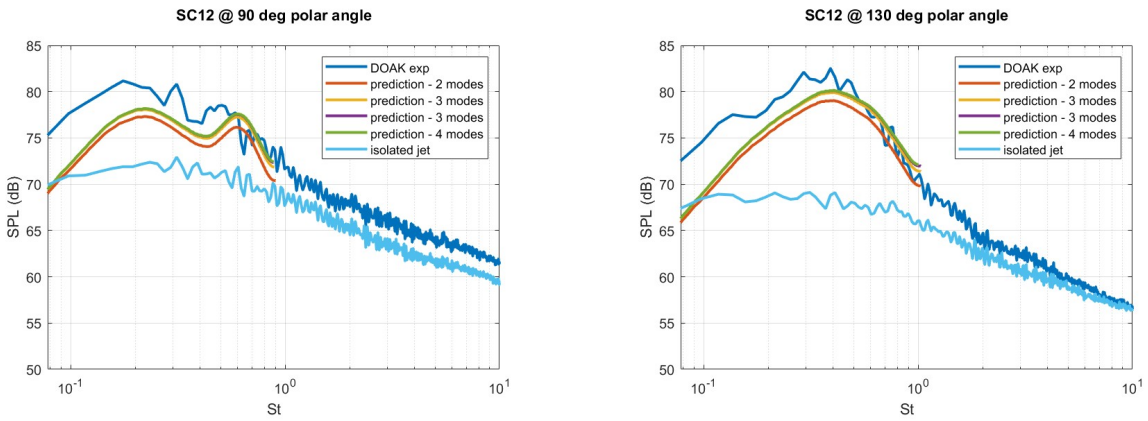

Fig. 2 Impact of the number of azimuthal modes used in the prediction of installed noise for nozzle SC12

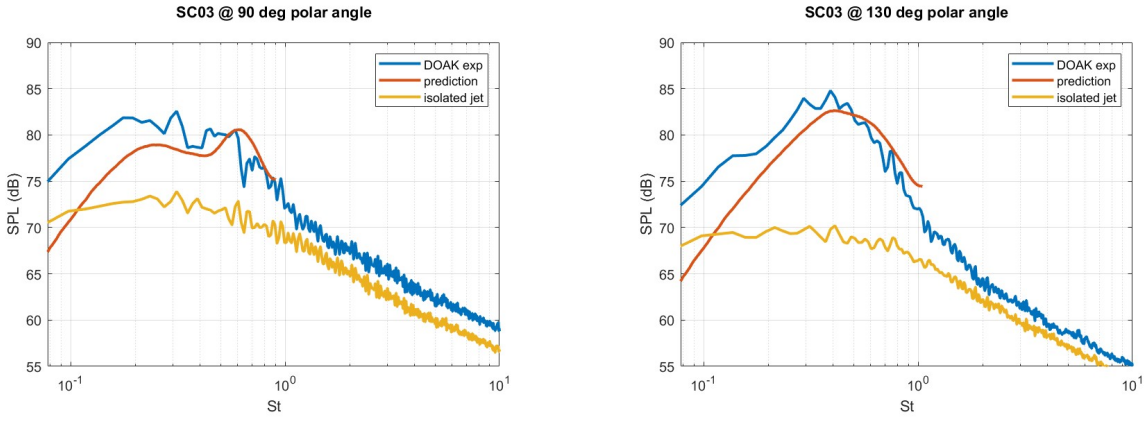

Fig. 3 Installed noise predictions versus experiments for nozzle SC03 - static case

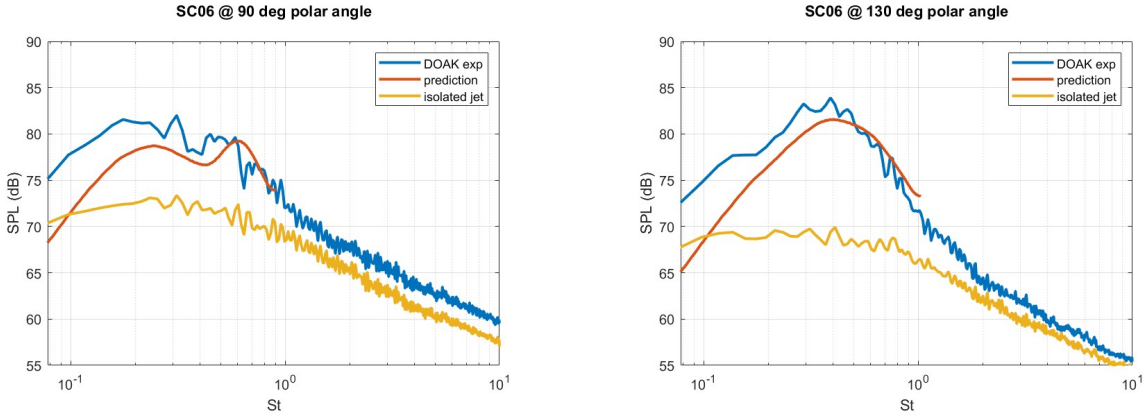

Fig. 4 Installed noise predictions versus experiments for nozzle SC06 - static case

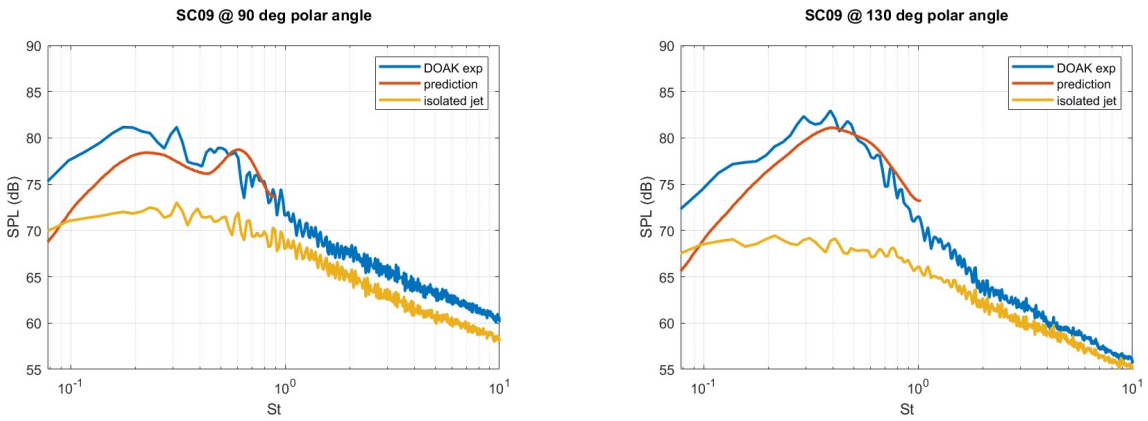

Fig. 5 Installed noise predictions versus experiments for nozzle SC09 - static case

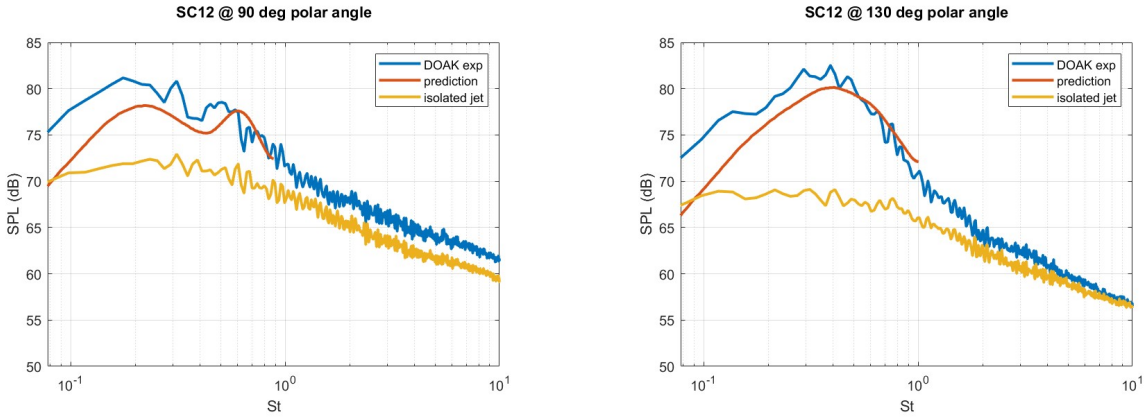

Fig. 6 Installed noise predictions versus experiments for nozzle SC12 - static case

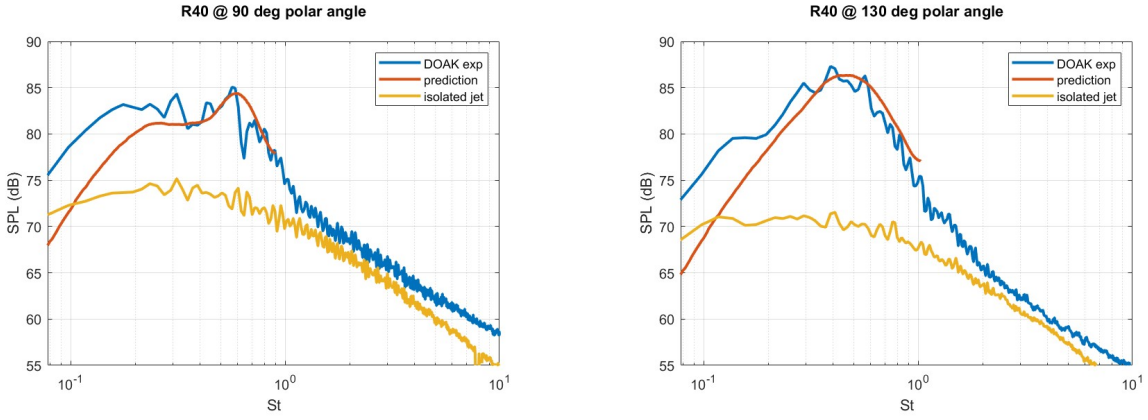

Fig. 7 Installed noise predictions versus experiments for round nozzle R40 - static case

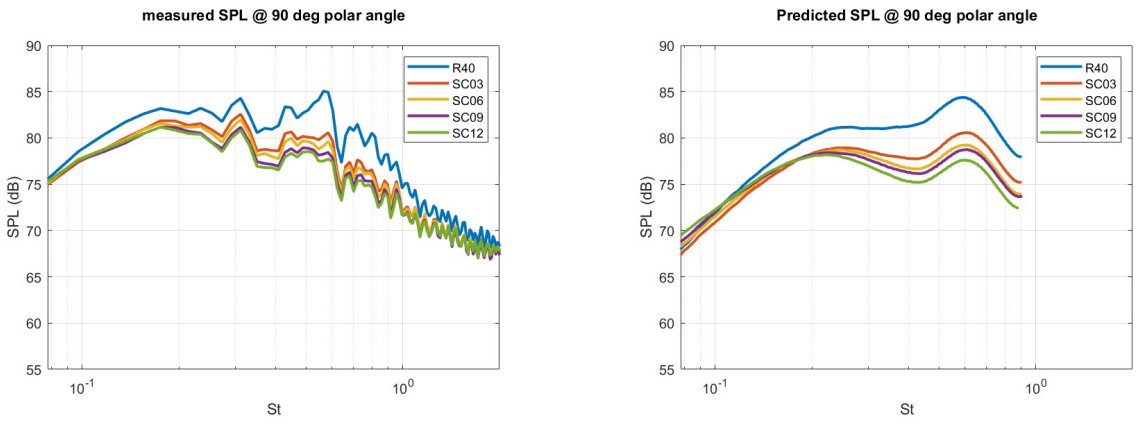

Fig. 8 Measured and predicted installed Sound Pressure Levels for all nozzles at $\theta = 90^o$ - static conditions

B. Predictions versus experiments for in-flight cases

The impact of the in-flight Mach number (M_f) on the installed noise is now under scrutiny, focusing particularly on $M_f = 0.1$. In accordance with Lyu and Dowling's model [8], the near-field is initially measured under static conditions, while the in-flight effects are subsequently incorporated into the scattering modeling.

Predictions for all the corrugated nozzles investigated in Section III.A and their respective experimental results are presented in Figures 9 to 13. In contrast to the static cases, the predictions tend to overestimate the installation noise by a maximum of 5 dB, typically at Strouhal numbers close to 0.6. A similar trend is observed for the round nozzle, as shown in Figure 14. However, it is worth noting that the numerical results are highly sensitive to the geometric variations of the nozzles. This sensitivity renders the model invaluable for swift comparisons between different designs or potential utilization in Multidisciplinary Optimization applications.

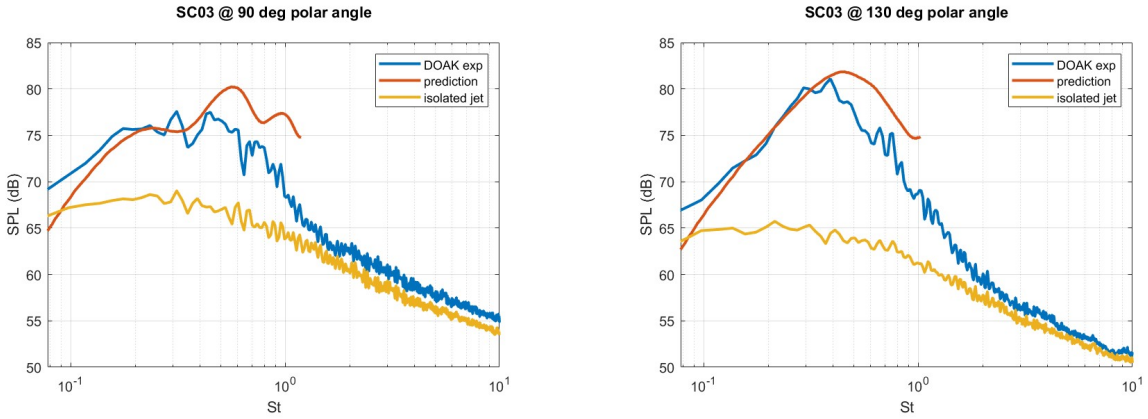

Fig. 9 Installed noise predictions versus experiments for nozzle SC03 - $M_f = 0.1$

IV. Conclusions

- Numerical results indicate a significant impact of the corrugations on the distribution of energy among modes, aligning with expectations.
- Lyu and Dowling's model has been effectively employed to predict the far-field Jet-Surface Interaction (JSI) noise of installed corrugated nozzles, exhibiting reasonable agreement with experiments conducted at the Doak Lab for both static and in-flight scenarios.

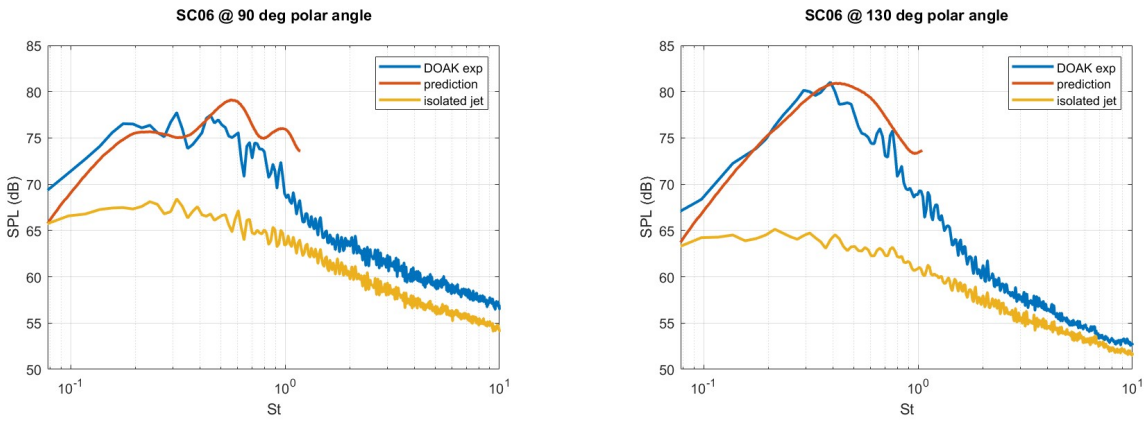

Fig. 10 Installed noise predictions versus experiments for nozzle SC06 - $M_f = 0.1$

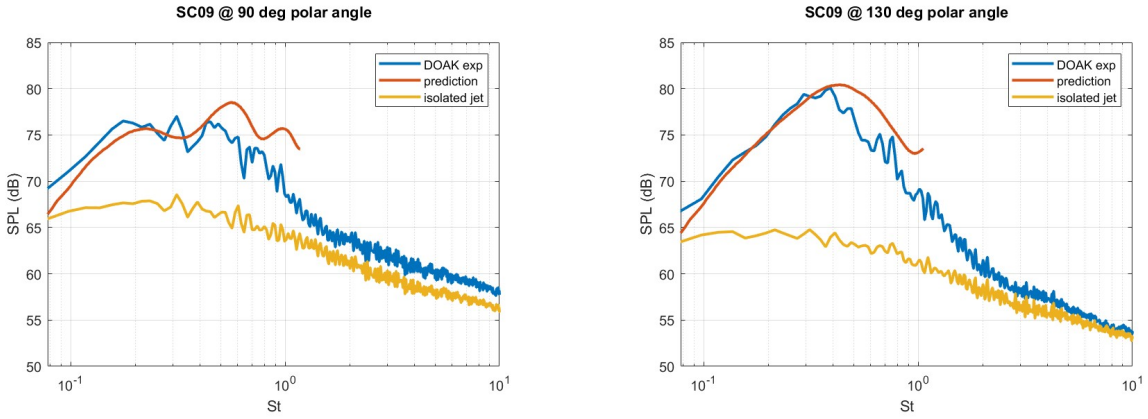

Fig. 11 Installed noise predictions versus experiments for nozzle SC09 - $M_f = 0.1$

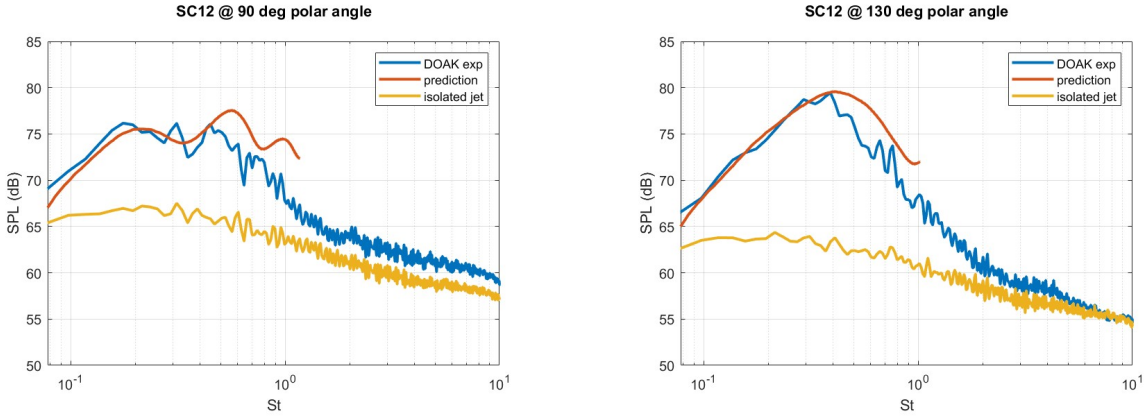

Fig. 12 Installed noise predictions versus experiments for nozzle SC12 - $M_f = 0.1$

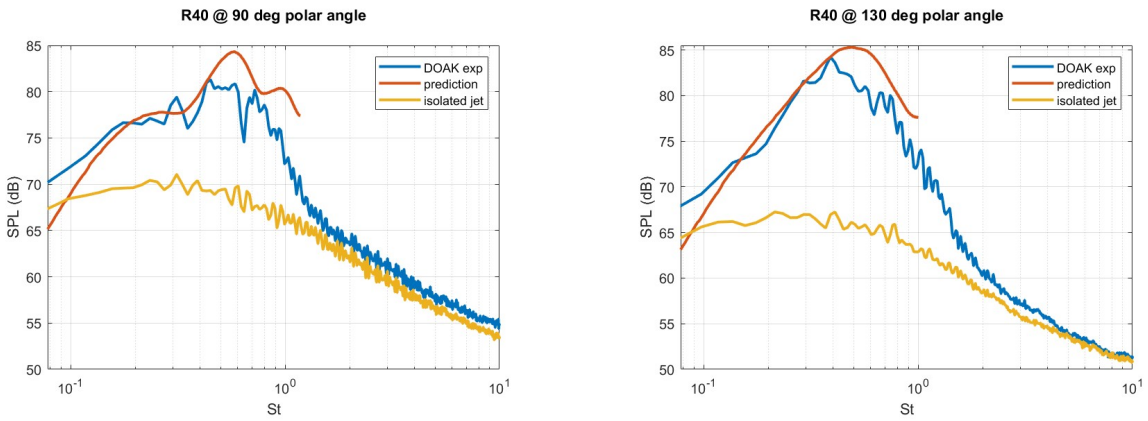

Fig. 13 Installed noise predictions versus experiments for round nozzle R40 - $M_f = 0.1$

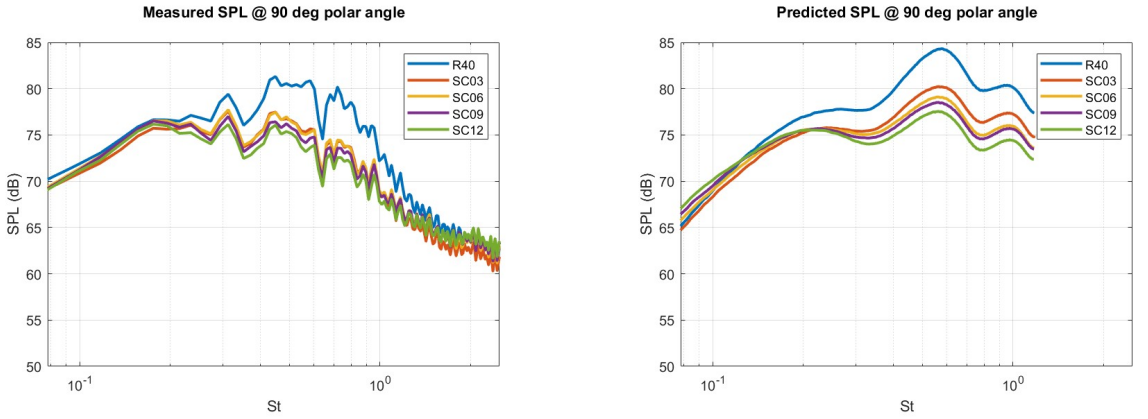

Fig. 14 Measured and predicted installed Sound Pressure Levels for all nozzles at $\theta = 90^o$ **-** $M_f = 0.1$

- Predictions for in-flight cases were observed to overestimate the installation noise. The reasons for this behavior remain unclear at this point, but it could be speculated that it is linked with the corrections used to account for in-flight effects in the near-field, and their association with possible inaccuracies in near-field measurements. Notably, a similar degree of over-prediction is observed for the equivalent round nozzle.
- Nonetheless, the model demonstrates sensitivity to the angle of corrugation in both static and in-flight scenarios, indicating its utility in swiftly evaluating variations in Sound Pressure Level (SPL) among different installed nozzle geometries.

V. Acknowledgements

This work is funded by the Innovate UK Research Programme FANTASIA - Future Aircraft Noise Technologies And Systems Integration Analytics (ref. 74217). The authors would also like to acknowledge the support provided by the Rolls-Royce University Technology Centre for Propulsion Systems Noise, within the Institute of Sound and Vibration Research at the University of Southampton. The first author would also like to thank the Federal University of Uberlandia.

References

[1] Alkislar, M. B., Krothapalii, A., and Butler, G. W., "The effect of streamwise vortices on the aeroacoustics of a Mach 0.9 jet," *Journal of Fluid Mechanics*, Vol. 578, 2007, p. 139–169. https://doi.org/10.1017/S0022112007005022.

[2] Zaman, K., Bridges, J., and Huff, D., "Evolution from 'Tabs' to 'Chevron Technology' - A Review," *International Journal of Aeroacoustics*, Vol. 10, No. 5-6, 2011, pp. 685–709. https://doi.org/10.1260/1475-472X.10.5-6.685, URL https://doi.org/10.1260/1475-472X.10.5-6.685.

[3] Wang, Z.-N., Tyacke, J. C., and Tucker, P. G., "LES–RANS Study of Serrated Nozzle Jet Aeroacoustics for an Installed Ultra-High-Bypass-Ratio Aeroengine," *AIAA Journal*, Vol. 59, No. 10, 2021, pp. 4155–4165. https://doi.org/10.2514/1.J060447, URL https://doi.org/10.2514/1.J060447.

[4] Samimy, M., Zaman, K. B. M. Q., and Reeder, M. F., "Effect of tabs on the flow and noise field of an axisymmetric jet," *AIAA Journal*, Vol. 31, No. 4, 1993, pp. 609–619. https://doi.org/10.2514/3.11594, URL https://doi.org/10.2514/3.11594.

[5] Bridges, J., Wernet, M., and Brown, C., "Control of jet noise through mixing enhancement," *Report No. NASA/TM-2003-212335*, 2003.

[6] Meyer, R., Kuo, C.-W., and McLaughlin, D. K., "Reduction of Subsonic Jet Noise by Passive Flow Control Devices," *19th AIAA/CEAS Aeroacoustics Conference*, 2013. https://doi.org/10.2514/6.2013-2147, URL https://arc.aiaa.org/doi/abs/10.2514/6.2013-2147.

[7] Proenca, A., and Lawrence, J., "Installed jet noise reduction using a zigzag vortex generator," *28th AIAA/CEAS Aeroacoustics 2022 Conference*, 2022. https://doi.org/10.2514/6.2022-2873, URL https://arc.aiaa.org/doi/abs/10.2514/6.2022-2873.

[8] Lyu, B., Dowling, A. P., and Naqavi, I., "Prediction of installed jet noise," *Journal of Fluid Mechanics*, Vol. 811, 2017, p. 234–268. https://doi.org/10.1017/jfm.2016.747.

[9] Proença, A., "Aeroacoustics of isolated and installed jets under static and in-flight conditions," Ph.D. thesis, University of Southampton, March 2018. URL https://eprints.soton.ac.uk/426880/.

[10] Dawson, M., "A Semi-Empirical Jet-Surface Interaction Noise Model," Ph.D. thesis, University of Southampton, April 2022.

Prediction of far-field noise from installed corrugated nozzles

de Souza, Francisco J.

2024-05-30

de Souza FJ, Lawrence J, Cruz RH, Proenca A. (2024) Prediction of far-field noise from installed corrugated nozzles. In: 30th AIAA/CEAS Aeroacoustics Conference (2024), 04-07 June 2024, Rome, Italy, Article number 2024-3310

https://doi.org/10.2514/6.2024-3310